SANDIA REPORT

SAND2003-1354
Unlimited Release
Printed April 2003

Growth and Characterization of Quantum Dots and Quantum Dots Devices

Jeffrey G. Cederberg, Robert M. Biefeld, H. Christian Schneider, Weng W. Chow

Prepared by
Sandia National Laboratories
Albuquerque, New Mexico 87185 and Livermore, California 94550

Sandia is a multiprogram laboratory operated by Sandia Corporation,
a Lockheed Martin Company, for the United States Department of Energy's
National Nuclear Security Administration under Contract DE-AC04-94AL85000.

Sandia National Laboratories

Issued by Sandia National Laboratories, operated for the United States Department of Energy by Sandia Corporation.

Available to DOE and DOE contractors from
U.S. Department of Energy
Office of Scientific and Technical Information
P.O. Box 62
Oak Ridge, TN 37831

Telephone: (865)576-8401
Facsimile: (865)576-5728
E-Mail: reports@adonis.osti.gov
Online ordering: http://www.doe.gov/bridge

Available to the public from
U.S. Department of Commerce
National Technical Information Service
5285 Port Royal Rd
Springfield, VA 22161

Telephone: (800)553-6847
Facsimile: (703)605-6900
E-Mail: orders@ntis.fedworld.gov
Online order: http://www.ntis.gov/help/ordermethods.asp?loc=7-4-0#online

SAND2003-1354
Unlimited Release
Printed April 2003

Growth and Characterization of Quantum Dots and Quantum Dots Devices

Jeffrey G. Cederberg, Robert M. Biefeld
Chemical Processing Science Department

H. Christian Schneider, Weng W. Chow
Semiconductor Material and Device Sciences Department

Abstract

Quantum dot nanostructures were investigated experimentally and theoretically for potential applications for optoelectronic devices. We have developed the foundation to produce state-of-the-art compound semiconductor nanostructures in a variety of materials: In(AsSb) on GaAs, GaSb on GaAs, and In(AsSb) on GaSb. These materials cover a range of energies from 1.2 to 0.7 eV. We have observed a surfactant effect in InAsSb nanostructure growth. Our theoretical efforts have developed techniques to look at the optical effects induced by many-body Coulombic interactions of carriers in active regions composed of quantum dot nanostructures. Significant deviations of the optical properties from those predicted by the "atom-like" quantum dot picture were discovered. Some of these deviations, in particular, those relating to the real part of the optical susceptibility, have since been observed in experiments.

Introduction

Compound semiconductor nanostructures have the potential to add an additional degree of freedom to the design of optoelectronic devices. In contrast to widely investigated two-dimensional confined systems, such as quantum wells, nanostructures, which exhibit additional confinement, have not been investigated sufficiently to allow nanostructures to be engineered into optoelectronic devices. This report discusses our progress in developing the experimental and theoretical base for future investigations of compound semiconductor nanostructures. This report is divided in two sections that represent the efforts involved with our investigations. The first part will discuss our experimental effort that involved the growth and characterization of nanostructures from several material systems by metal-organic chemical vapor deposition (MOCVD). The second part will discuss our theoretical effort to look at the optical properties of semiconductor nanostructures and their potential use as active regions for semiconductor lasers.

Experimental efforts in the growth of compound semiconductor nanostructures

Several material systems have the potential to form nanostructures, due to the strain between the deposited layer and the substrate. Our initial efforts considered the conditions under which InAs nanostructures could be formed on GaAs. Conditions for InAs QD growth by MOCVD on GaAs substrates were established. Optimum conditions for QD growth were determined from AFM measurements and PL measurements. The AFM images in Figure 1 illustrate the formation of InAs islands as the amount of InAs deposited increases.

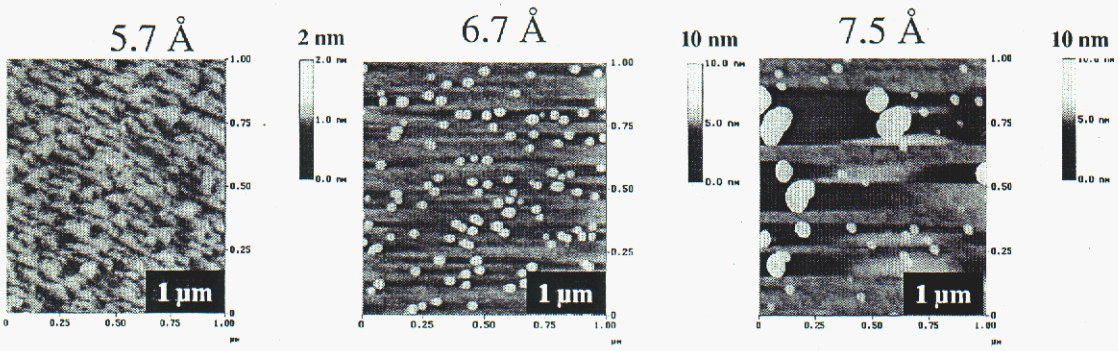

Figure 1. AFM images of InAs on GaAs showing the evolution of InAs islands. Amounts of InAs for each image are listed above the image. For further discussion see text.

Increasing the amount of InAs above 6.7 Å causes the islands to coalesce, forming larger islands. The islands grow larger, both in lateral dimension and in height, while their density decreases. InAs nanostructures show strong photoluminescence at room temperature ranging over energies from 1.2 to 1.0 eV that depend on the size of the nanostructure. Large islands have lower energy emission due to reduced quantum confinement. Multilayer stacks of quantum dots might be incorporated into laser diodes. We have observed a factor of ten increase in the emission from a five period structure compared to a single layer of nanostructures.

Growth conditions for GaSb/GaAs QD grown by MOCVD were established. Optimum conditions for QD growth were determined from AFM measurements. The growth of GaSb/GaAs nanostructures is more robust and reproducible than the InAs/GaAs system. Figure 2 shows the formation islands after the deposition of 15 Å of GaSb as the growth temperature is varied. Islands formed at 500°C have a density of 100 μm^{-2} and have a rectangular base of 70 nm by 30 nm and a height of 2 nm. In contrast to InAs nanostructures on GaAs, GaSb nanostructures on GaAs have almost no optical activity even at measurement temperatures of 4 K. This is probably due to evaporation of

the nanostructure when the antimony partial pressure is removed from the reactor for the growth of a GaAs capping layer.

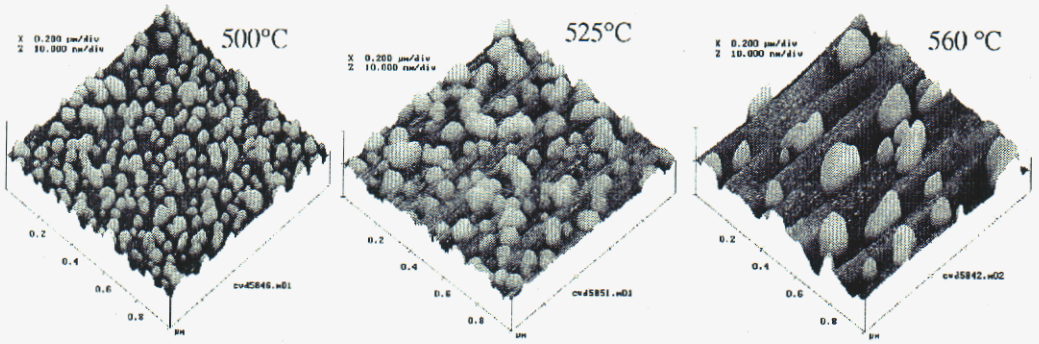

Figure 2. AFM images of GaSb on GaAs showing the evolution of GaSb islands as the growth temperature changes. Growth temperature is listed above each image. For further discussion see text.

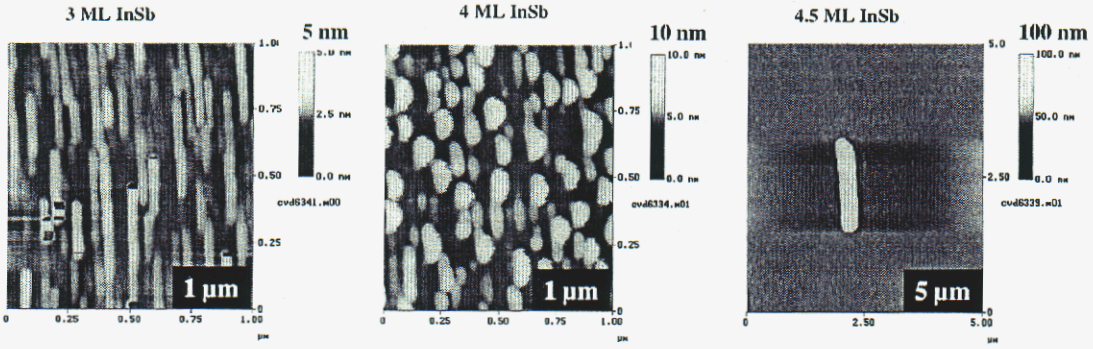

Figure 3. AFM images of InSb on GaSb showing the evolution of InSb islands. Amounts of InSb for each image are listed beside the image. For further discussion see text.

InSb nanostructures on GaSb were investigated as an extension of our work. The sensitivity of the nanostructure size distribution to the amount of InSb deposited is similar to the case of InAs on GaAs. Figure 3 shows the average island size for 4 ML of InSb is 140 nm long, 40 nm wide, and 3 nm high. Larger islands form within an additional 0.5 ML of the smaller islands. InSb quantum dots have shown emission out as far as 0.73 eV

During our investigations the unexpected observation of a "surfactant" effect on the formation of III-V nanostructures was made. The addition of antimony to InAs, forming a dilute alloy InAs(Sb), results in dramatic transformations of the nanostructures. In a complementary experiment, As is added to InSb to form a dilute alloy In(As)Sb, which also dramatically changes the island size and density distributions. The growth of semiconductor nanostructures by MOCVD requires an understanding of the initial nucleation of deposits. Using reactor growth studies coupled with *ex situ* sample analysis by Atomic Force Microscopy (AFM), we have conducted a detailed investigation of these two different material systems: InAs on GaAs(001) and InSb on GaSb(001). These films are predicted to nucleate by the Stranski-Krastanov (SK) mechanism, forming nanometer-sized islands in a two-dimensional wetting layer. The strong surfactant effect is a surprise. Small (35 x 20 nm, 2 nm high), dense (300 μm^{-2}) islands are formed for 9 Å-thick InAs grown on GaAs(001), that are elongated towards the [1-10] direction. (see Figure 4) The addition of antimony results in the coalescence of small islands into long, wire-like structures that are elongated in the perpendicular direction, i.e., in the [110] direction. Isolated islands can be formed for the InAs(Sb) alloy by decreasing the deposit thickness to 7.5 Å. The islands thus formed are larger than InAs structures, and are still elongated in the [110] direction. Looking at the complementary case of InSb on GaSb(001), we see the formation of very large (140 x 40 nm, 2 nm high) islands under all of the growth conditions that were investigated. The addition of As to form In(As)Sb produces smaller (50 x 20 nm, 1 nm high), and more dense (90 μm^{-2}) islands. The alloyed structures are smaller than the pure InSb islands grown under the same conditions. Clearly the minority constituent has a pronounced effect on the mechanism of island

nucleation. Our proposed explanation is due to the weaker bonding of antimony compared to arsenic. The addition of antimony to an arsenic-terminated surface may increase the diffusion length of adatoms and decrease the surface energy. Conversely, the addition of arsenic to antimony-terminated surfaces may decrease the diffusion length and increase the surface energy. The nucleation of nanostructures by self-assembled mechanisms, such as the SK morphology transformation, is governed largely by the film properties that are only controlled in a gross way via growth settings. We have shown, by the addition of small amounts of a dilute component, that this transformation can be adjusted. Species that form stronger bonds result in smaller islands, while species with weaker bonds allow faster and more facile diffusion, which results in larger islands. These observations suggest a way to manipulate the size and dimensions of nucleated islands, or force a nucleated layer to wet a substrate surface more rapidly.

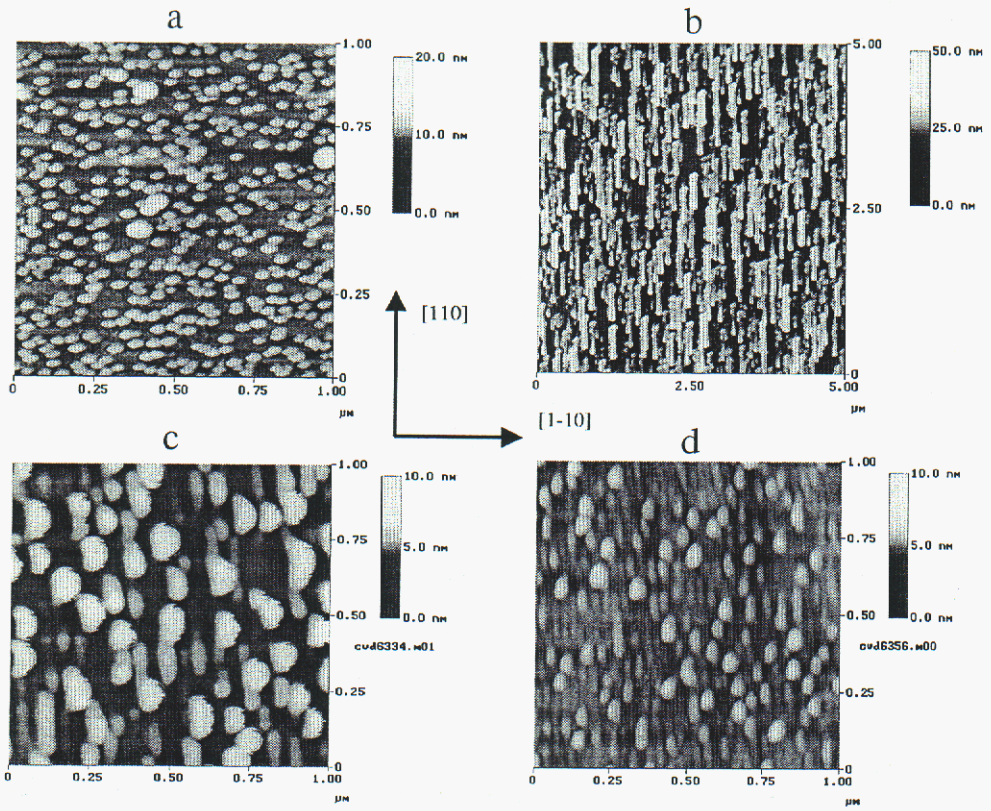

Figure 4. Atomic Force Microscope images showing the effects of antimony and arsenic additions to InAs and InSb quantum dot structures, respectively. (a) AFM showing InAs islands on a GaAs substrate. (b) The addition of Sb during the growth of InAs on GaAs results in larger elongated islands. (c) InSb islands on a GaSb substrate are initially large with a wide size distribution. (d) The addition of As during the growth of InSb on GaSb results in smaller, more uniform islands.

Theoretical modeling of quantum dots lasers diodes

Insight into the physics of optoelectronic devices based on semiconductor nanostructures was developed using theoretical techniques. Self-organized quantum-dot materials are presently investigated theoretically both for their unusual electronic structure as well as for their applications to quantum-dot lasers. Because these quantum dots exhibit bound states, their electronic structure is often described as that of an "artificial" atom. However, important differences between atomic systems and quantum dots remain: The bound states of electrons and holes in quantum dots are different from their atomic counterparts because of the dot shapes and strain fields which are created during the growth process. The continuum states with energies greater than the dot confinement energies are not scattering states for dissociated electrons and protons, as is the case for atoms, but resemble extended two-dimensional quantum-well states because the quantum dots are either grown inside of a quantum well or are connected to a wetting layer. When these quantum-well states are populated, they decisively influence the optical and transport properties of quantum-dot systems.

A theory was developed for an active quantum dot structure. To ensure the applicability of the theory for conditions involving high output power or high speed switching, we use a self-consistent treatment of the coupled quantum dot/quantum well system, including many-body Coulomb effects. Our approach involves adapting the semiconductor Bloch equations in the screened Hartree-Fock approximation to describe a shallow quantum dot surrounded by a quantum well region. This picture describes both strain-induced dots and dot-in-a-well structures. The solution of the semiconductor Bloch equations gives the optical spectra.

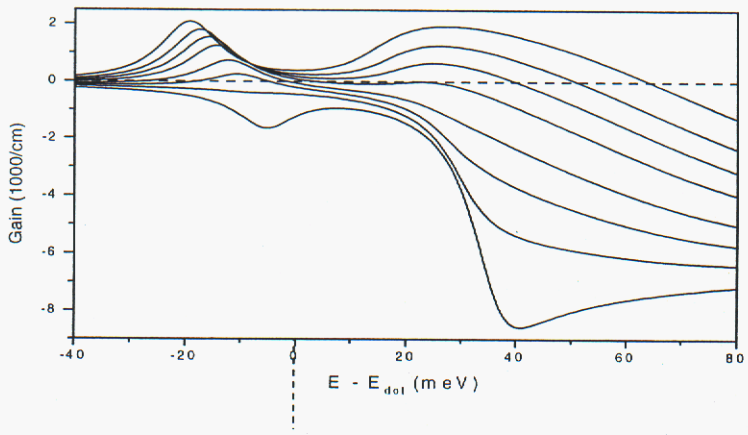

Figure 5. Computed gain spectra for combined quantum-dot/quantum well system at 300 K. The two-dimensional density of quantum dots in the well is $n_{dot} = 10^{11}cm^{-2}$. The total carrier densities are 3.0, 5.0, 6.5, 8.0 X $10^{11}cm^{-2}$, and 1.0, 1.3, 1.50 X $10^{12}cm^{-2}$. The zero of the energy scale corresponds to the dot transition-energy at zero carrier density.

Figure 5 shows computed gain spectra for a range of carrier densities. The figure shows how the absorption of the discrete dot transition changes with increasing carrier density into gain. Similarly, the absorption due to the quantum-well states shows the familiar signature of an excitonic resonance at lower carrier densities and changes to gain with sufficiently high carrier density. The Coulomb interaction leads to self-energy shifts for the quantum-dot and quantum-well transitions. An important feature of these shifts is that the relative shift is not rigid, resulting in a reduction in the energy separation between the quantum-dot and quantum-well states with increasing carrier densities. A consequence is the redistribution of the carrier population in the quantum dot and quantum well states, which in turn can alter the carrier relaxation times. We theoretically investigated the excitation dependence of the optical properties of quantum dots. The investigation showed that the Coulomb coupling of the localized discrete states in the quantum dots to continuum states results in carrier density dependencies of gain and refractive index. These dependencies differ significantly from those predicted for an

isolated quantum-dot description where many-body Coulomb effects and the interaction with the surrounding quantum-well region are neglected. For example, Figure 6 shows that the present theory predicts values ranging from -1 to 2 for the α factor (linewidth enhancement factor, or antiguiding factor) under typical lasing conditions. Negative α factors at the gain peak do not exist for quantum-well and bulk lasers, and have important implications for the phase-front properties of the laser field. In particular, the break-up (or filamentation) of the laser beam in the lateral direction in broad-area quantum-well lasers is due to the positive linewidth enhancement factor exhibited by conventional active regions. This filamentation tendency severely limits the high-power single-mode output of quantum-well and bulk semiconductor lasers. Since a high-power single-mode output is highly desirable for a wide variety of applications, the deviation from this behavior, which we found for quantum dots, is important for semiconductor-laser engineering.

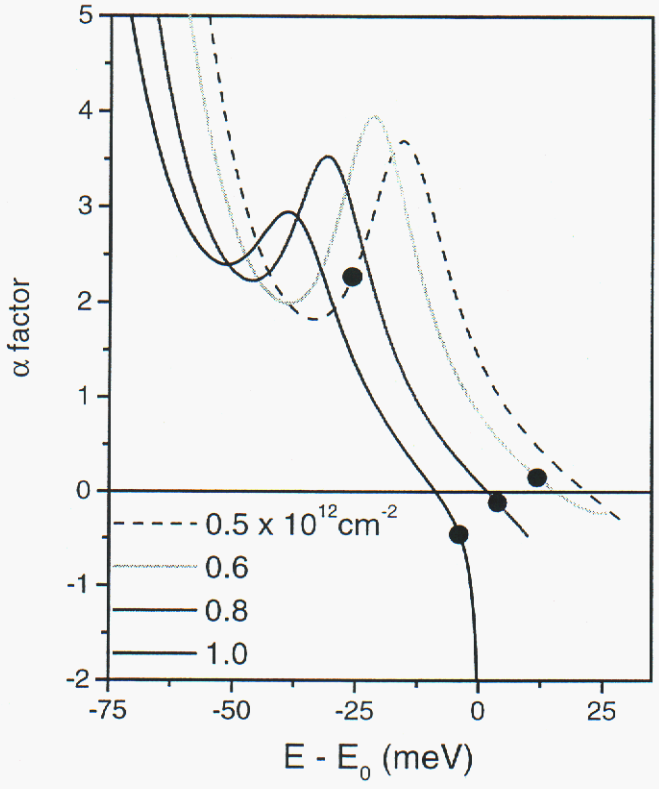

Figure 6. Antiguiding factor α vs. energy for sheet carrier densities of 0.5, 0.6, 0.8 and $1.0\times10^{12}cm^{-2}$. The energy is measured from the quantum-dot ground-state resonance at zero excitation. The dots mark the antiguiding factor at the gain peak.

The theory was applied to describe the experimental results on the filamentation tendency in quantum-dot lasers (experiments performed at Cardiff University, UK). The study involves the measurement of the near field linewidth of broad area lasers with quantum dot and quantum well active regions designed to emit at 1 μm. Figure 7 shows that the quantum dot devices exhibit less filamentation than comparable quantum well devices and exhibit a reduction in filamentation as the injection level is increased. This is consistent with our theory and calculated results that includes the Coulomb coupling between dot and wetting-layer states on a microscopic level and predicts a linewidth enhancement factor from –3 to 1, depending on carrier density and inhomogeneous broadening.

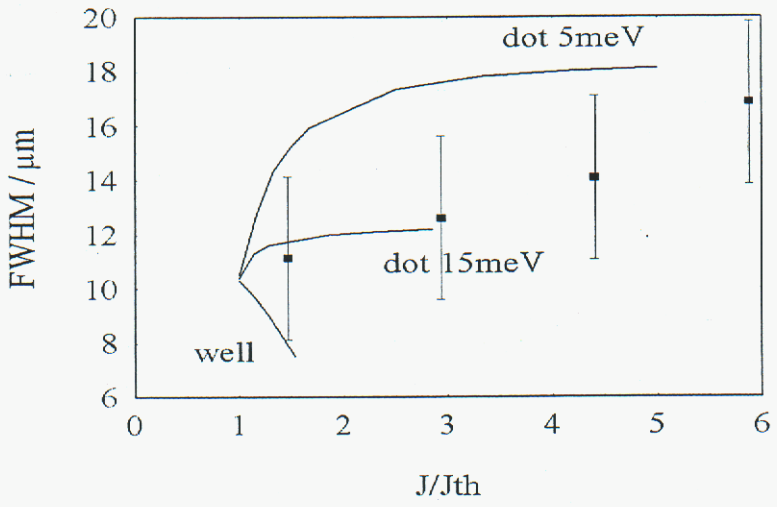

Figure 7. Computed filament full width at half maximum for a stripe device of length 500μm containing a quantum well (lower curve) and quantum dots with inhomogeneous broadening widths of 5 and 15meV (upper and middle curves respectively) as a function of drive current relative to threshold. Values derived from the experimental data for 550 μm long quantum dot devices are shown as points.

Conclusions

We have developed the foundation to produce state-of-the-art compound semiconductor nanostructures in a variety of materials: In(AsSb) on GaAs, GaSb on GaAs, and In(AsSb) on GaSb. These materials cover a range of energies from 1.2 out to 0.73 eV. We have observed a surfactant effect on nanostructure growth. Larger islands are produced when Sb is added to InAs and smaller islands form when As is added to InSb.

Our theoretical efforts led to a microscopic theory for quantum dot lasers. In this theory the optical effects induced by many-body Coulombic interactions of carriers in active regions are taken into account. The many-body Coulomb interactions result in effects in a quantum dot active medium that does not follow the often-used "atom-like" description. The deviations predicted by our theory have been verified by experiments.

Appendix, LDRD Summary

Referred publications resulting from the work:

H. C Schneider, W. W. Chow and S. W. Koch, 'Anomalous Carrier Induced Dispersion in Quantum Dot Active Media', Phys. Rev. B, Vol. 66, 041210, (2002).

P.M. Smowton, E.J. Pearce, H.C. Schneider, W.W. Chow, and M. Hopkinson, 'Filamentation and Linewidth enhancement factor in InGaAs Quantum Dot Lasers', Appl. Phys. Lett., Vol. 81, 3251, (2002).

W. W. Chow and H. C. Schneider, 'Theory of Laser Gain in InGaN Quantum Dots', Appl. Phys. Lett., Vol. 81, 2566, (2002).

H.C. Schneider, W.W. Chow, S.W. Koch, 'Many-body effects in the gain spectra of highly excited quantum-dot lasers', Phys. Rev. B, Vol. 64, 5315, (2001).

H.C. Schneider, W.W. Chow, P.M. Snowton, E.J. Pearce, S.W. Koch, "Anomalous carrier-induced dispersion in semiconductor quantum dots", to be published in 'Optics in 2002', special issue, Optics Photonics New, Dec. 2002.

J.G. Cederberg, R.M. Biefeld, 'Growth of InAsSb Quantum Dots on GaAs(100)', submitted to Appl. Phys. Lett., (2002).

All other reports and publications from the work: 1

Number of Patent Disclosures: 0

Number of Staff Hired: 1

Number of Applications: 0

Number of Post Docs: 2

Number of Patents: 0

Number of Students: 1

Number of Copyrights: 0

Number of Awards (and their names): 0

Initial Distribution

Org.	Name	MS
1100	J.M. Phillips	MS 1427
1111	B.L. Doyle	MS 1056
1112	J.C. Barbour	MS 1415
1112	N.A. Modine	MS 1415
1114	N.D. Shinn	MS 1415
1118	G.N. Hayes	MS 1423
1118	M.C. Phillips	MS 1423
1118	R.J. Foltynowicz	MS 1423
1122	G.A. Samara	MS 1421
1122	P.P. Provencio	MS 1421
1123	J.A. Simmons	MS 0601
1123	W.W. Chow	MS 0601
1123	E.D. Jones	MS 0601
1123	S.R. Kurtz	MS 0601
1123	M.P. Lilly	MS 1415
1123	S.K. Lyo	MS 1415
1123	K.E. Waldrip	MS 0601
1126	R.M. Biefeld	MS 0601
1126	J.G. Cederberg (4)	MS 0601
1126	M.E. Coltrin	MS 0601
1126	F.H. Kaatz	MS 0601
1126	G. Wang	MS 0601
1141	P.V. Dressendorfer	MS 1413
1742	G.M. Peake	MS 0601
Qty		
1	Central Technical Files, 8945-1	MS 9018
2	Technical Library, 9616	MS 0899
1	For DOE/OSTI	MS 0612